nature communications

Article

https://doi.org/10.1038/s41467-023-39900-9

Optimal reactive nitrogen control pathways identified for cost-effective $PM_{2.5}$ mitigation in Europe

Received: 9 February 2023

Accepted: 30 June 2023

Published online: 17 July 2023

Check for updates

Zehui Liu[1,2], Harald E. Rieder[3], Christian Schmidt[3], Monika Mayer[3], Yixin Guo[1,2], Wilfried Winiwarter[2,4] ✉ & Lin Zhang[1] ✉

Excess reactive nitrogen (Nr), including nitrogen oxides (NO_x) and ammonia (NH_3), contributes strongly to fine particulate matter ($PM_{2.5}$) air pollution in Europe, posing challenges to public health. Designing cost-effective Nr control roadmaps for $PM_{2.5}$ mitigation requires considering both mitigation efficiencies and implementation costs. Here we identify optimal Nr control pathways for Europe by integrating emission estimations, air quality modeling, exposure-mortality modeling, Nr control experiments and cost data. We find that phasing out Nr emissions would reduce $PM_{2.5}$ by 2.3 ± 1.2 μg·m^{-3} in Europe, helping many locations achieve the World Health Organization (WHO) guidelines and reducing $PM_{2.5}$-related premature deaths by almost 100 thousand in 2015. Low-ambition NH_3 controls have similar $PM_{2.5}$ mitigation efficiencies as NO_x in Eastern Europe, but are less effective in Western Europe until reductions exceed 40%. The efficiency for NH_3 controls increases at high-ambition reductions while NO_x slightly decreases. When costs are considered, strategies for both regions uniformly shift in favor of NH_3 controls, as NH_3 controls up to 50% remain 5-11 times more cost-effective than NO_x per unit $PM_{2.5}$ reduction, emphasizing the priority of NH_3 control policies for Europe.

Ambient $PM_{2.5}$ (fine particulate matter with an aerodynamic diameter ≤2.5 μm) air pollution is one of the leading risk factors for premature mortalities worldwide, according to the Global Burden of Disease (GBD) study[1], responsible for millions of deaths and lost years of healthy life annually in recent years[1–3]. Long-term policies for $PM_{2.5}$ mitigation have been implemented in many countries and have effectively reduced $PM_{2.5}$ concentrations[4–7]. However, large numbers of people are still exposed to harmful $PM_{2.5}$ levels even in places with relatively clean ambient air such as Europe[7]; 59% of European stations exceed the World Health Organization (WHO) guideline for the $PM_{2.5}$ annual mean (10 μg·m^{-3}) in 2019[8]. Recent epidemiological studies also demonstrated that $PM_{2.5}$ air pollution can affect human health at very low levels[9,10]. The WHO thus released an updated guideline value for $PM_{2.5}$ annual mean concentrations (5 μg·m^{-3})[3], which was exceeded at 97% of European monitoring stations in 2019[8]. This poses a tremendous challenge for cleaning up European air as much more stringent mitigation measures will be needed to achieve such an ambitious goal. The WHO also suggested interim targets to be considered, although recognizing that interim targets are insufficient to remove adverse health impacts.

Excess reactive nitrogen (Nr), including nitrogen oxides (NO_x = NO + NO_2), ammonia (NH_3), nitrate (NO_3^-), and ammonium (NH_4^+) are recognized environmental threats to ecosystems, deteriorating the quality of air, soil, and water[11,12]. Anthropogenic Nr sources have dramatically increased since 1960[13], exacerbating the global nitrogen cycle and consequent damaging effects on human health and

[1]Laboratory for Climate and Ocean-Atmosphere Studies, Department of Atmospheric and Oceanic Sciences, School of Physics, Peking University, Beijing 100871, China. [2]International Institute for Applied Systems Analysis (IIASA), A-2361 Laxenburg, Austria. [3]Institute of Meteorology and Climatology, Department of Water, Atmosphere and Environment, University of Natural Resources and Life Sciences (BOKU), A-1180 Vienna, Austria. [4]Institute of Environmental Engineering, University of Zielona Góra, PL 65-417 Zielona Góra, Poland. ✉e-mail: winiwart@iiasa.ac.at; zhanglg@pku.edu.cn

ecosystems[13,14]. Capping anthropogenic Nr emissions (mainly NO_x and NH_3) is a high priority for environmental protection[15,16]. In particular, Nr controls benefit $PM_{2.5}$ mitigation because both NO_x and NH_3 are precursors of secondary inorganic aerosols (SIAs, including sulfate, nitrate, and ammonium) components in $PM_{2.5}$, apart from sulfur dioxide (SO_2)[14,17,18]. SIAs strongly contribute to the $PM_{2.5}$ mass concentrations in Europe[19–21], contributing above 50% of total annual $PM_{2.5}$ mass concentrations in parts of Europe, i.e., Germany, the Netherlands, and Belgium[22–24]. Atmospheric abundance of NH_3 and NO_x gases determine the formation of SIAs, and effectiveness of $PM_{2.5}$ mitigation from Nr controls[25–27]. NH_3 preferably reacts with sulfuric acid (H_2SO_4, produced by the oxidation of SO_2) to form ammonium sulfate aerosol, and with more NH_3 available, further reacts with nitric acid (HNO_3, produced by the oxidation of NO_x) to form ammonium nitrate aerosol.

The revised Gothenburg Protocol has set national Nr emission ceilings for 2020, i.e., 42% NO_x emission reductions and 6% NH_3 emission reductions in 2020 relative to 2005 for the European Union (EU)[28] and other participating countries. The National Emissions Ceiling Directive further establishes national Nr emission reduction targets in 2030, i.e., 63% NO_x emission reductions and 19% NH_3 emission reductions in 2030 relative to 2005 in the EU[29]. All existing national targets show more ambitious controls for NO_x than NH_3. Most countries have not prioritized limiting NH_3 emissions in part due to uncertainties in NH_3 sources and concerns about its control effectiveness for $PM_{2.5}$ mitigation, in addition to food security concerns[17], with agriculture being the dominant source of NH_3. However, recent studies found agricultural (mainly NH_3) emissions make the largest relative contribution to $PM_{2.5}$ mortality in Europe among all sources[2,30,31]. Gu et al. [18] also found that the cost of 50% NH_3 emissions abatement is much less than that of NO_x emissions globally. However, the priority for NO_x or NH_3 emission reductions to meet the updated WHO guideline and zero pollution action plan[32] in Europe remains uncertain.

In this study, we quantify the contribution and efficiency of Nr emission reductions for $PM_{2.5}$ mitigation in Europe for 2015 and derive the optimal pathway for Nr emission controls. We use recent European emission estimates, a regional air quality model, the newly developed exposure mortality model, Nr control scenarios, and emission control costs to systematically analyse the impact of Nr emission controls on $PM_{2.5}$ air pollution (Methods). We demonstrate that Nr emission controls can reduce $PM_{2.5}$ concentrations, $PM_{2.5}$-related health impacts, and help achieve the WHO guideline in Europe. The optimal pathway targeting $PM_{2.5}$ abatement changes towards prioritizing NH_3 measures after considering control costs, indicating NH_3 emission reductions are the most cost-effective way to combat European $PM_{2.5}$ air pollution.

Results and discussion

The contribution of Nr emissions on $PM_{2.5}$ air pollution

Our ECLIPSE inventory derived from the GAINS (Greenhouse gas and Air pollution Interactions and Synergies) model (Methods) estimates the total anthropogenic NO_2 and NH_3 emissions over Europe in 2015 to be 3.7 Tg N and 4.4 Tg N, respectively, which are comparable to other emission inventories (Supplementary Table 1). Considering monthly time factors, NH_3 emissions tend to peak during the warm season (April-September), while NO_x emissions peak during the cold season in Europe. Such seasonality appears stronger in our estimates than in the EDGAR and EMEP inventories (Supplementary Fig. 1). Both NH_3 and NO_x emissions are higher in the western part of Europe than in the east. This ECLIPSE emissions inventory is used as an input to the Weather Research and Forecasting model coupled with Chemistry (WRF-Chem) regional air quality model to assess the impacts of Nr emission reductions on $PM_{2.5}$ air pollution in Europe. A series of WRF-Chem simulations are conducted over Europe for the representative months (January, April, July, and October) in 2015 (Methods). The baseline simulation in Europe, after improving simulated organic carbon (OC) and dust by matching observations of $PM_{2.5}$ components (Supplementary Figs 2 and 3), well captures measured surface $PM_{2.5}$ concentrations with the correlation coefficients (R) > 0.59 and mean bias (MB) < −6% (Supplementary Fig. 3). The magnitudes and variations of the observed SIAs concentrations are generally captured by the baseline simulation, except in summer, when the model underestimates nighttime nitrate volatility and overestimates nitrate concentrations. The simulated surface annual NH_3 concentrations are also in good agreement with measurements in Europe with R = 0.92 and MB of within −3% (Supplementary Fig. 4).

The contribution of anthropogenic Nr emissions to $PM_{2.5}$ air pollution can be calculated as the difference between the baseline simulation and a sensitivity simulation with anthropogenic Nr emissions set to zero (Methods). Figure 1 shows that the reduction in regional annual mean $PM_{2.5}$ concentrations when phasing out anthropogenic Nr emissions is $2.3 \pm 1.2\ \mu g \cdot m^{-3}$ (mean ± standard deviation) in Europe for 2015. The response to such emission controls for $PM_{2.5}$ concentrations is stronger in Western Europe than in Eastern Europe, with the largest effects occurring in the Netherlands, Belgium and northern Germany. For evaluation, we separate Europe into Western Europe and Eastern Europe along country borders, guided by the spatial difference of $PM_{2.5}$ changes from Nr emission controls (the thick black line in Fig. 1). We further apply a metric of N-share[18] to quantify the contribution of Nr compounds to total $PM_{2.5}$ concentrations, which is defined as the relative change in model simulated $PM_{2.5}$ concentrations with vs. without anthropogenic Nr emissions. The N-share caused by anthropogenic Nr emissions contributes about 29% (range, 17–31%) to $PM_{2.5}$ pollution in Western Europe and 12% (8.7–16%) in Eastern Europe for 2015, exceeding 50% in some parts of Western Europe. The N-shares of NH_3 emissions are larger than those of NO_x emissions and close to the N-shares of total Nr emissions because the NH_3 reductions curtail both contributions of NO_x and SO_2 to SIAs formation, which is in agreement with results of Gu et al.[18].

Nr abatement would help Europe to achieve the limit set in the updated WHO guidelines for $PM_{2.5}$ concentrations and substantially mitigate $PM_{2.5}$-related health burdens. In 2015, only 14% of Western Europe met the $PM_{2.5}$ annual mean $<5\ \mu g \cdot m^{-3}$ (the updated WHO guideline value) and all of Eastern Europe exceeded this guideline level. Figure 2 shows that phasing out Nr emissions prompt an additional 28% of Western Europe to achieve the guideline value for annual mean $PM_{2.5}$. NH_3 emission controls render twice as much area in Western Europe meeting the guideline value compared to similar strengths of NO_x emission controls. However, annual mean $PM_{2.5}$ concentrations in Eastern Europe cannot reach this guideline value with Nr abatement alone and need to reduce emissions of other $PM_{2.5}$ precursors. In addition, Western Europe and Eastern Europe have 18% and 38% of all days in 2015 exceeding the guideline value for the daily average $PM_{2.5}$, and Nr abatement cuts the daily exceedance by 41% and 16% respectively. The Global Exposure Mortality Model (GEMM) is then applied to assess $PM_{2.5}$-related chronic health impacts (Methods). We further find setting anthropogenic Nr emissions to zero could avoid 99,000 (95% confidence interval: 92,000-106,000) $PM_{2.5}$-related premature deaths in Europe in 2015, decreasing the annual $PM_{2.5}$-related mortality by 29% and 6% in Western Europe and Eastern Europe, respectively (Supplementary Fig. 5).

The efficiency of Nr emission reductions in Europe

The analyses above illustrate a larger contribution of NH_3 emissions to $PM_{2.5}$ concentrations, and that phasing out NH_3 emissions leads to larger areas and more days meeting the updated WHO guideline value for $PM_{2.5}$ air pollution compared to phasing out NO_x. We further investigate the effectiveness of Nr emission controls under different reduction levels in sensitivity simulations with NH_3 and NO_x emission reductions of 0%, 30%, 60%, 80%, and 100% over Europe in 2015 (Methods). We should note such reduction strengths extend to very

https://doi.org/10.1038/s41467-023-39900-9

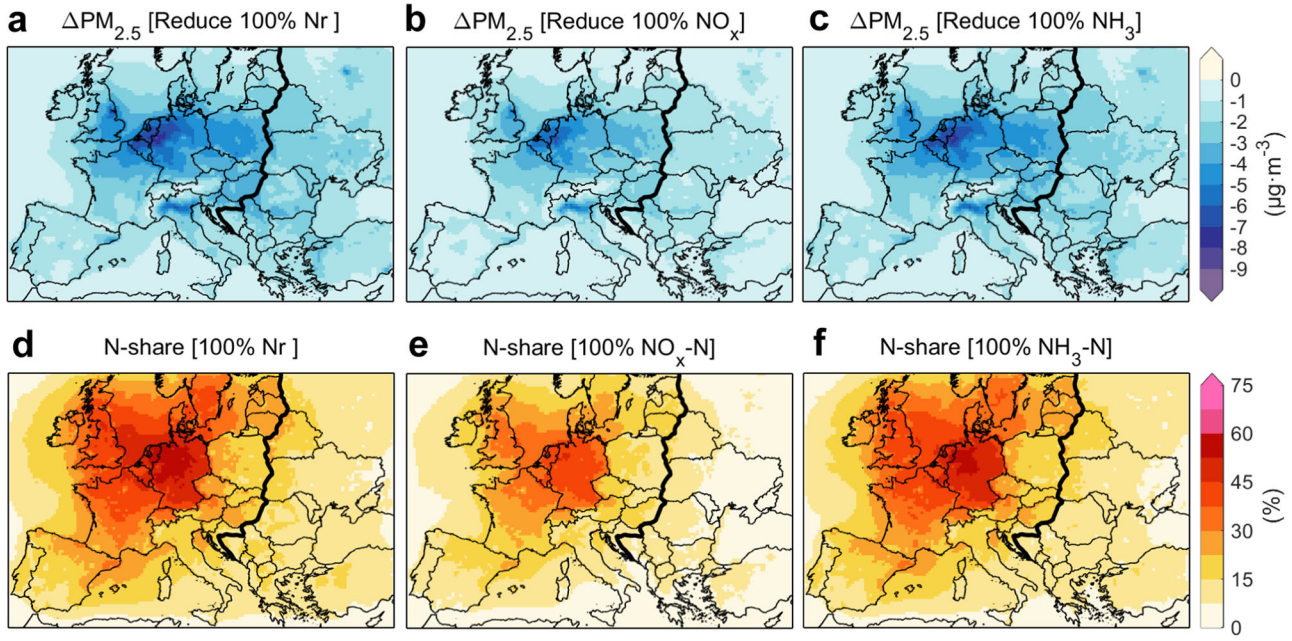

Fig. 1 | Contribution of reactive nitrogen (Nr) emissions to $PM_{2.5}$ air pollution over Europe in 2015. a–c Changes of $PM_{2.5}$ concentrations induced by phasing out anthropogenic Nr (NO_x + NH_3) emissions (**a**), NO_x emissions (**b**), and NH_3 emissions (**c**) respectively. **d–f** N-shares of $PM_{2.5}$ air pollution associated with Nr (**d**), NO_x (**e**), and NH_3 (**f**) emissions.

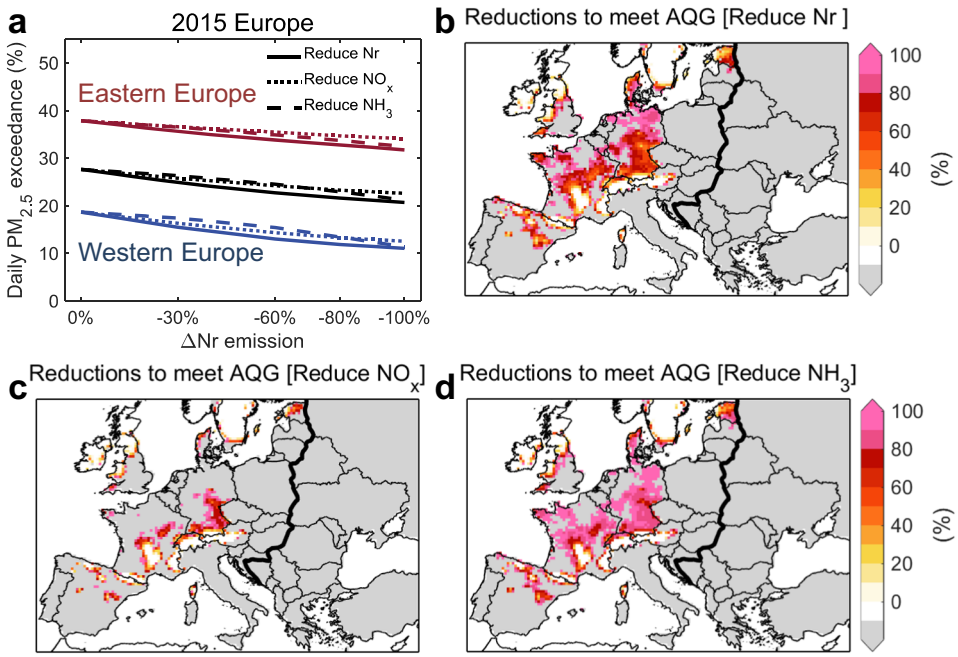

Fig. 2 | Impacts of reactive nitrogen (Nr) emission controls on the World Health Organization (WHO) air quality guideline (AQG) achievement. a Changes in regional mean daily WHO AQG (15 μg·m^{-3}) $PM_{2.5}$ level exceedance when European Nr (solid lines), NO_x (long dash lines), and NH_3 (short dash lines) emissions are gradually decreased in 2015. **b–d** the reduction in Nr (**b**), NO_x (**c**), NH_3 (**d**) emissions required to meet the WHO AQG for annual mean $PM_{2.5}$ (5 μg·m^{-3}). Blue, red, and black lines in (**a**) represent changes of regional mean daily $PM_{2.5}$ exceedance in Western Europe, Eastern Europe, and all Europe, respectively. Gray areas in (**b**), (**c**), and (**d**) represent locations where even 100% Nr emission controls cannot lead to achievement.

drastic changes of atmospheric conditions that, while currently not seeming realistic, guide the way towards conditions compatible with the WHO guideline values and provide the information needed to devise efficient abatement.

Figure 3 shows changes in regional mean $PM_{2.5}$ concentrations and related premature deaths in Western Europe and Eastern Europe as anthropogenic Nr emissions are gradually reduced. In Western Europe, the $PM_{2.5}$ concentrations decline non-linearly following NH_3 emission reductions, resulting in modest $PM_{2.5}$ changes with limited NH_3 emission reductions, which is similar to the response found in China[26]. The regional mean $PM_{2.5}$ concentrations in Western Europe for 2015 would decrease by 0.40 ± 0.15/1.03 ± 0.41/2.51 ± 1.06 μg·m^{-3} with 30%/60%/100% NH_3 emission reductions in Europe. Only a deep NH_3 abatement (up to about 80%) would yield larger total $PM_{2.5}$ decreases

https://doi.org/10.1038/s41467-023-39900-9

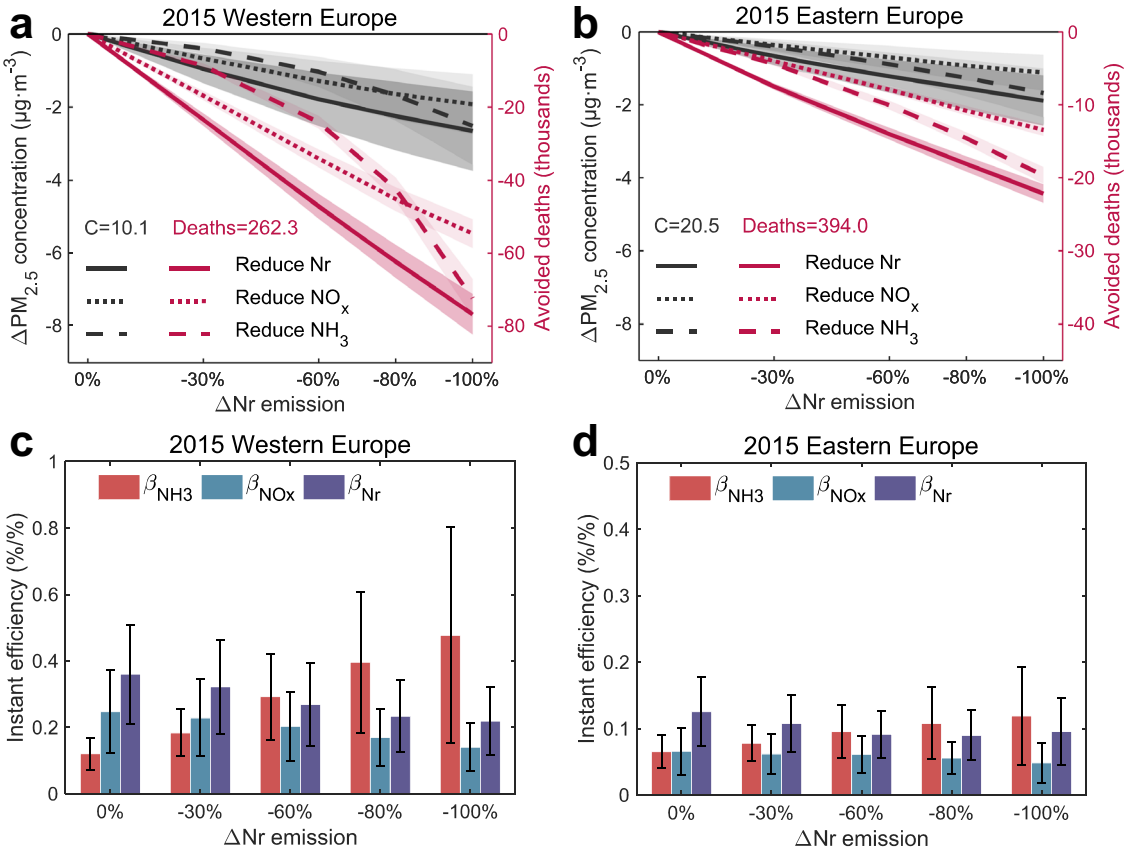

Fig. 3 | Effectiveness of reactive nitrogen (Nr) emission reductions in Europe in abating regional mean surface $PM_{2.5}$ air pollution in 2015. a, **b** Reductions in Western Europe (**a**) and Eastern Europe (**b**) annual mean $PM_{2.5}$ concentrations (black lines), and $PM_{2.5}$-related premature deaths (red lines) when European Nr (solid lines), NO_x (long dash lines), and NH_3 (short dash lines) emissions are gradually abated in 2015. **c**, **d** changes in Western Europe (**c**) and Eastern Europe (**d**) annual mean instant efficiency (refers the instant response of $PM_{2.5}$ in percentage to 1% reduction in Nr emissions under each Nr emission scenario) associated with Nr (purple bars), NO_x (green bars), and NH_3 (red bars) emission controls. The baseline simulated regional annual mean $PM_{2.5}$ concentrations (denoted as "C"), and $PM_{2.5}$-related premature deaths (denoted as "Deaths") are shown in (**a**) and (**b**). Shading in (**a**) and (**b**) represent values (means ± one spatial standard deviation) of $PM_{2.5}$ concentrations or $PM_{2.5}$-related premature deaths. Vertical bars in (**c**) and (**d**) represent values (means ± one spatial standard deviation) of instant efficiency.

in Western Europe than the same level of NO_x abatement. We note a difference to previous studies[33,34] that expect higher efficiency for NH_3 already at a much lower level of abatement, which we understand to be the result of a change in the chemical regime since these earlier studies were performed. While $PM_{2.5}$ decreases in Eastern Europe associated with NH_3 emission reductions tend to be more linear than those in Western Europe, the responses are similar to NO_x emission reductions. Notably, during summer, both regions exhibit a more linear relationship between $PM_{2.5}$ concentrations and NH_3 emission reductions, primarily due to the greater availability of HNO_3 compared to other seasons (Supplementary Fig. 6). Meanwhile, we find stronger non-linear responses on $PM_{2.5}$-related premature deaths in both regions due to the non-linear relationship between health risk and $PM_{2.5}$ exposure; their values can be decreased by 8.7 (8.0–9.3)/24 (22–26)/72 (67–78) thousands $PM_{2.5}$-related premature deaths in Western Europe for 2015 when NH_3 emissions are reduced by 30%/60%/100%.

We quantify the effectiveness for $PM_{2.5}$ reductions by calculating the instant efficiency of Nr emission controls (β, Methods). $\beta_{Nr}/\beta_{NOx}/\beta_{NH3}$ estimates the instant response of total $PM_{2.5}$ mass in percent for each 1% mass reduction in $Nr/NO_x/NH_3$ emissions. As shown in Fig. 3, the regional mean β_{NH3} increases rapidly while β_{NOx} slowly decreases as the level of emission reduction rises. Under the 2015 emission condition, the β_{NH3} efficiencies in Western Europe increase from 0.12 ± 0.05%/% in the base condition to 0.48 ± 0.33%/% (a factor of 4 higher) when NH_3 emissions are reduced by 80%, while the β_{NOx} efficiencies decrease from 0.25 ± 0.13%/% to 0.14 ± 0.07%/%. The efficiencies in Eastern Europe are less than half of those in Western Europe due to the higher $PM_{2.5}$ concentrations and lower N-share (Fig. 1), and are less sensitive to Nr emission changes.

We then apply the chemical regime metric of G ratio[25] to explain the changes in the instant efficiency associated with NH_3 emission controls. The G ratio denotes the ratio between free ammonia (NH_3 and NH_4^+) and total nitrate ($HNO_3 + NO_3^-$) after neutralization of H_2SO_4 (note, all the terms are expressed on a molar basis, Methods). The 2015 mean G ratio is found to be almost always above 1 across Europe (4.5 ± 2.4 in Western Europe and 2.8 ± 1.7 in Eastern Europe), indicating a HNO_3-limited chemical regime and causing the SIAs formation to be more sensitive to small changes in NO_x emissions than those in NH_3 emissions (Supplementary Fig. 7). This phenomenon is particularly evident in April (with a G ratio of 6.3 ± 3.2 in Western Europe and 4.2 ± 2.0 in Eastern Europe) due to the high ammonia emissions occurring in Europe during this month. In contrast, the G ratio is close to 1 in most of Eastern Europe for January, July, and October, when NH_3 controls are slightly more efficient than NO_x controls (Supplementary Fig. 6). The G ratio decreases as we gradually reduce NH_3 emissions and Europe shifts to the NH_3-limited chemical regime, leading to NH_3 abatement becoming increasingly effective (Supplementary Fig. 8). When we gradually reduce NO_x emissions, Europe remains in the HNO_3-limited chemical regime but the β_{NOx} decreases due to decreases in oxidants (Supplementary Figs. 8 and 9). Changes in β_{Nr} depend on both β_{NOx} changes and shifts in the chemical regime. This results in a slow decrease of β_{Nr} in Western Europe and a trend of first decreasing

and then increasing in Eastern Europe with deeper emission reductions.

A tipping point for the Nr controls can be identified where the $PM_{2.5}$ response from NH_3 emission reductions outweighs that from NO_x emission reductions, i.e., by interpolating β_{NH3}–β_{NOx} or G–1 to reach zero among a series of NH_3 and NO_x abatement sensitivity tests (Methods). We find that the β_{NH3}–β_{NOx} tends to be positive as Nr emissions are reduced, and it has larger changes in the places with more excessive NH_3 (Supplementary Fig. 10). Figure 4 shows the tipping point of Nr emission reductions for instant efficiencies are 36% ± 16% and 18% ± 22% in Western Europe and Eastern Europe, respectively. It indicates small mitigation for NH_3 or NO_x can decrease the same $PM_{2.5}$ concentrations in Western Europe after around 36% emission reductions in 2015. However, the G ratios are still above 1 under these abatement scenarios, and the tipping point for G ratio = 1 needs a deeper NH_3 abatement (73% ± 16% in Western Europe and 46% ± 24% in Eastern Europe). The discrepancies between metrics of the chemical regime for SIAs formation and the effectiveness for $PM_{2.5}$ decreases are also found in Thunis et al.[35].

We find the first explanation for the discrepancy between the tipping point from β efficiency and that from the G ratio would be the different unit of Nr abatement, the former indicating the same $PM_{2.5}$ decreases with per 1% mass reduction of Nr emissions and the latter indicating per unit mole reduction. This discrepancy is reduced by 36–41% when we transfer the unit of β from mass-based to molar-based. The residual discrepancy can be explained by their different definitions and applicable targets. The G ratio is based on a homogeneous air parcel at any specific moment and it loses extreme values when applied to the regional air quality model. As shown in Fig. 4, the tipping point for the G ratio falls rapidly with height while β changes steadily. Therefore, the decrease of surface $PM_{2.5}$ depends on the chemical regime of each specific grid cell and time interval. This demonstrates that the instant efficiency is more suitable for evaluating Nr emission controls for $PM_{2.5}$ mitigation while the chemical regime only provides a rough direction.

The optimal pathway for Nr abatement in Europe

Here, we develop and apply a diagnostic diagram for the effectiveness of $PM_{2.5}$ abatement to find the optimal pathway of Nr emission controls in Europe (Methods). It visualizes the regional mean $PM_{2.5}$ reductions as isopleths and the combined instant efficiency for $PM_{2.5}$ abatement (the gradient) as arrows. As shown in Fig. 5, the gradient in Western Europe for the 2015 base condition tends to shift towards NO_x, which indicates that NO_x emission controls would initially be most effective. By contrast, for Eastern Europe NH_3 and NO_x emission controls have the similar effects in the early stage. Following the direction of gradients, we find that the optimal pathway of Nr emission controls in Western Europe entails always stronger reductions in NO_x than NH_3 emissions so that the regional mean $PM_{2.5}$ concentrations decline the fastest. This pathway approaches to reductions of ~100% NO_x emissions and 40% NH_3 emissions inducing $PM_{2.5}$ decreases by 2.2–2.4 μg·m^{-3}, and further NH_3 emission reductions will lead to an additional 0.4 μg·m^{-3} decrease. In contrast, the optimal pathway of Nr emission controls in Eastern Europe shall have a deeper NH_3 abatement where ~100% NH_3 and 60% NO_x emission reductions result in $PM_{2.5}$ decreases by 1.7–1.9 μg·m^{-3}.

In addition to $PM_{2.5}$ abatement, cost considerations are also essential information for policy-making. Here we note that the optimal pathway of Nr emission controls changes uniformly in favor of NH_3 emission reductions when we consider control costs. We quantify Nr emission abatement technologies and related costs (including investment costs, fixed and operating costs) according to the GAINS model[36–38]. Figure 5 shows the annual total costs for Nr abatement in Western Europe and Eastern Europe according to integration and interpolation among five sets of feasible emission control scenarios at the national level reported by Amann et al.[39]. Here, the costs refer to the extra annual costs incurred by the individual abatement measures to reduce Nr emissions. The abatement measures for NO_x emissions stem mainly from the power and industrial sectors, while those for NH_3 are mainly from agricultural livestock farming and fertilizer use. We find NH_3 emission controls are always cheaper than NO_x emission controls and Western Europe has higher costs to control Nr emissions than Eastern Europe due to the reduction policies already in place and higher levels of Nr emissions. Currently feasible emission abatement technologies in the GAINS model can reduce NO_x and NH_3 emissions by 16% and 29% in Western Europe, annually costing 3.7 and 0.8 billion euros, respectively; reduce NO_x and NH_3 emissions by 32% and 31% in Eastern Europe, annually costing 1.9 and 0.2 billion euros, respectively.

We further update the diagnostic diagram of cost-effectiveness using the ratio of control costs and $PM_{2.5}$ abatement, which denotes the annual costs per unit $PM_{2.5}$ decreases (Fig. 5). Due to the limited availability of cost data for high abatement levels, we merely extrapolate to 50% emission reductions. In Western Europe, controlling 10% (30%) NH_3 emissions from the 2015 Base would decrease regional $PM_{2.5}$ by 0.11 (0.40) μg m^{-3} and require implementation costs of 0.08 (1.1) billion euros. In comparison, controlling 10% (30%) NO_x emissions there would decrease regional $PM_{2.5}$ by 0.23 (0.67) μg m^{-3} with implementation costs of 1.1 (12.7) billion euros. Similar cost-effective NH_3 emission controls can be seen in Eastern Europe. The optimal pathway of cost-effective Nr emission controls follows the lowest isopleths for the cost/$PM_{2.5}$ abatement ratio, inferring NH_3 emission reductions only in both Western Europe and Eastern Europe. The much lower cost and increasing efficiency of NH_3 emission control diminish the need for NO_x emission control.

Nr emission controls thus can help Europe towards achieving the updated WHO guideline value, reducing $PM_{2.5}$ air pollution by 12–29% and $PM_{2.5}$-related mortality by 6–29% in Europe in 2015. Eastern Europe (G ratios of 1–5) represents an area slightly in excess of NH_3 where modest NO_x or NH_3 emission reductions abate similar $PM_{2.5}$ concentrations. In contrast, Western Europe (G ratios of 2–7) represents a highly NH_3-excessive area where $PM_{2.5}$ abatement does not become effective until NH_3 reduction reaches above 40%. When considering control costs, the optimal pathway for halving Nr emissions clearly points towards NH_3 management. Policy challenges specific to NH_3 abatement have been described recently by Gu et al. [40]. Identifying the optimal pathway for Nr emission reductions combining the effectiveness of $PM_{2.5}$ abatement and emission control costs may also be important in many other regions over the globe, such as China, India, and the United States, where nitrogen pollution has continued to grow in recent years[41–43]. These regions are also facing heavy loads of $PM_{2.5}$ air pollution and challenges to meet the updated WHO guideline value[7,44]. In addition to the benefits for $PM_{2.5}$ mitigation and human health, Nr emission controls can also help reduce nitrogen deposition and surface ozone (Supplementary Fig. 9), which should be integrally considered in environmental strategies in future work.

In closing, we note that some uncertainties are associated with our analyses. First, several emission inventories based on different sectoral categories and collected by different institutions provide a considerable range of Nr emission estimates in Europe. While the estimates we use are within the range (Supplementary Table 1), the net results will be affected by the choice of Nr input. Second, the availability of NH_3 may significantly elevate the aerosol water content and alkalinity and then enhance the production of SIAs and SOA[45,46]. The contribution of NH_3 emissions on $PM_{2.5}$ air pollution would thus present a lower estimate only, as here, the alkalinity is limited to the heterogeneous production of SIAs, and the SOA formation is parameterised as a multiple of OC concentrations. Furthermore, our study has not included the bidirectional exchange of NH_3, i.e., simultaneous fluxes from and deposition to agricultural areas, which is highly uncertain and may alter the effectiveness of $PM_{2.5}$ mitigation[47,48].

https://doi.org/10.1038/s41467-023-39900-9

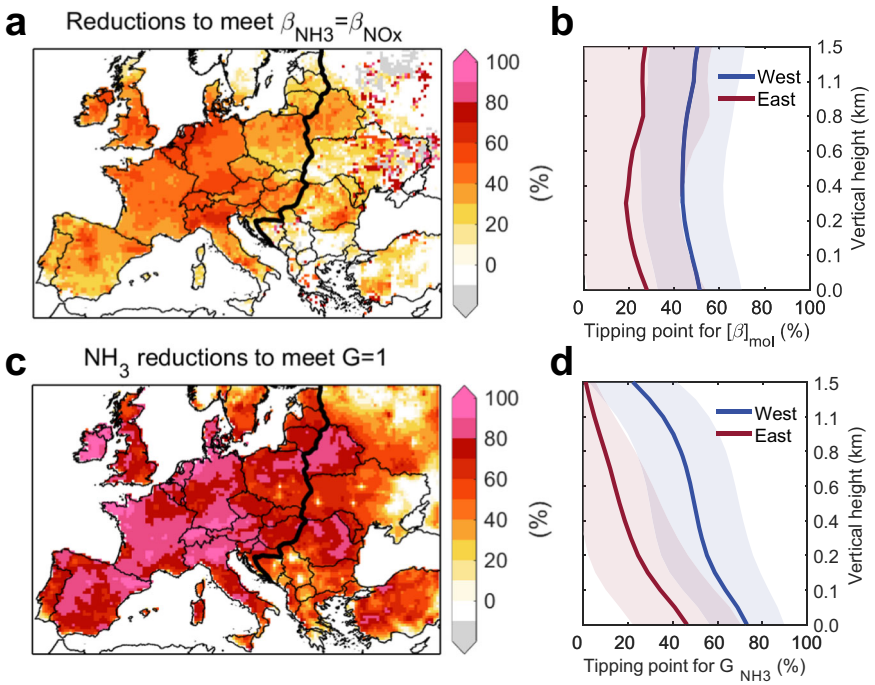

Fig. 4 | Tipping point of reactive nitrogen (Nr) emission control effectiveness targeting $PM_{2.5}$ abatement. a, **c** Tipping point for surface $PM_{2.5}$ response from NH_3 emission reductions outweighs that from NO_x emission reductions identified by $\beta_{NH3} = \beta_{NOx}$ (**a**) and the NH_3 saturation ratio G = 1 (G, the ratio between free ammonia (NH_3 and NH_4^+) and total nitrate ($HNO_3 + NO_3^-$) after neutralization of H_2SO_4) (**c**). **b**, **d** Vertical profiles of Western Europe (red) and Eastern Europe (blue) mean tipping point for $\beta_{NH3} = \beta_{NOx}$ (**b**) and G = 1 (**d**). Gray areas in (**a**), and (**c**) represent that 100% Nr emission controls here cannot achieve the tipping point. Shading in (**b**) and (**d**) represent values (means ± one spatial standard deviation) of tipping point.

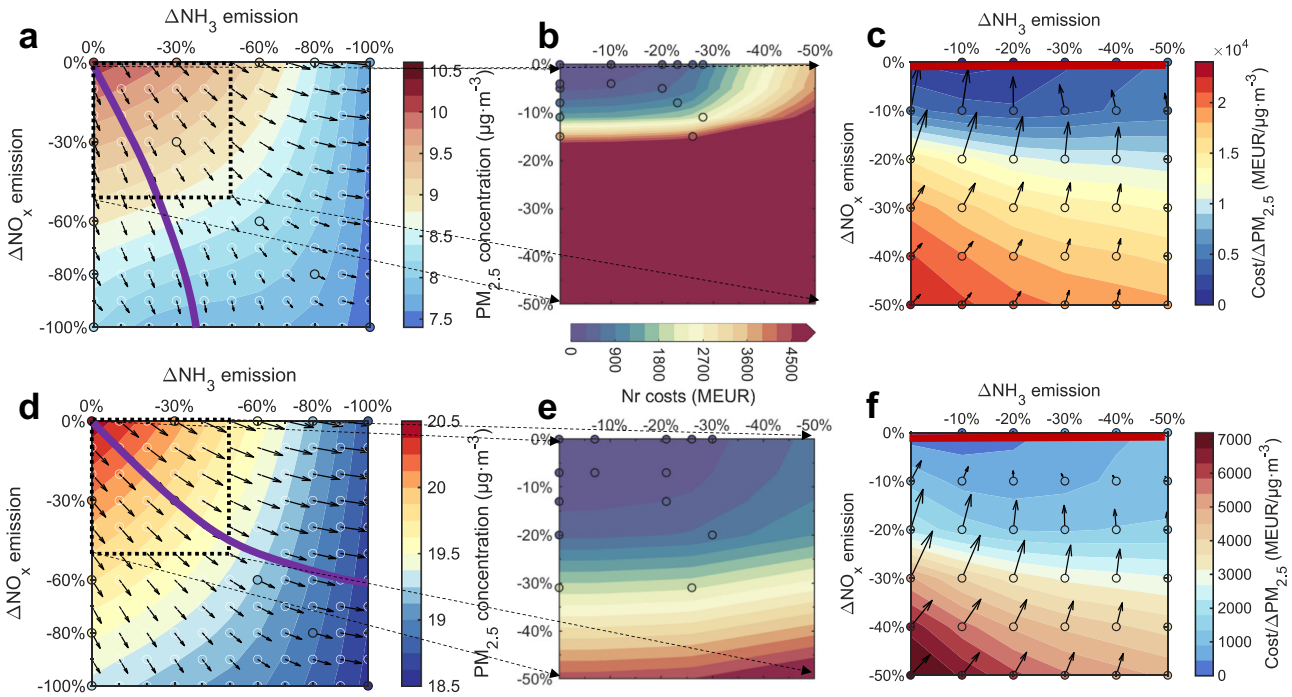

Fig. 5 | Diagnostic diagram to identify the optimal pathway of reactive nitrogen (Nr) emission controls towards effective $PM_{2.5}$ abatement and minimal control costs. a, **d** the diagnostic diagram for effectiveness of regional annual mean $PM_{2.5}$ abatement to find the optimal pathway (purple line) of Nr emission controls in Western Europe (**a**) and Eastern Europe (**d**). **b**, **e** Control costs for Nr emissions according to the NH_3 (*x*-axis) and NO_x (*y*-axis) emission changes from 0 to 50% in Western Europe (**b**) and Eastern Europe (**e**). **c**, **f** the diagnostic diagram for the ratio of control costs and $PM_{2.5}$ abatement to find the optimal pathway (red line) of Nr emission controls in Western Europe (**c**) and Eastern Europe (**f**). Black, white circles, and black arrows in (**a**) and (**d**) show 13 sets of simulated regional mean $PM_{2.5}$ concentrations, interpolated $PM_{2.5}$ concentrations, and their gradients in the diagnostic diagram. Black circles in (**b**) and (**e**) show control costs from five sets of feasible scenarios in the GAINS model. Black circles and arrows in (**c**) and (**f**) show the ratio of control costs and $PM_{2.5}$ abatement at each 10% control level and their gradients in the diagnostic diagram.

Methods

Observations of air pollutants and meteorology

Daily and hourly surface chemical measurements in Europe in 2015 are obtained from the air quality database of the European Environment Agency (EEA). We use 964 background stations for $PM_{2.5}$, which are then spatially aggregated into 565 grid cells to get a more representative evaluation of the model results. In addition, we use 27 stations for BC, 30 stations for OC, 34 stations for SIAs (Supplementary Table 2), and 21 stations for NH_3. Of these, 26 stations containing all $PM_{2.5}$ components are used to improve model SOA. Meteorological observations at 2072 stations in Europe in 2015 are collected from the National Climatic Data Center (NCDC), which consists of hourly 10-m wind speed (WS10), 10-m wind direction (WD10), 2-m air temperature (T2), and 2-m relative humidity (RH2). Evaluations of baseline simulated meteorology with these observations generally show good agreement (Supplementary Table 3).

The WRF-Chem model

Model configuration. The Weather Research and Forecasting model coupled with Chemistry (WRF-Chem) version 4.0.3 is applied to simulate the meteorology and $PM_{2.5}$ concentrations. The model domain includes most European countries and their surrounding regions using 150 (east-west) × 100 (south-north) grid cells at a 27-km spatial resolution. We divide the vertical atmosphere into 38 levels, with a first layer height of 10 meters above ground and a top pressure of 5000 Pa. The initial and lateral meteorological boundary conditions are based on hourly datasets from the European Centre for Medium-Range Weather Forecasts (ECMWF) Integrated Forecasting System (IFS) with a spatial resolution of 0.25°[49]. We nudge every 2-day meteorological fields with ERA5 reanalysis data to keep actual atmospheric conditions. The chemical initial and boundary conditions are driven by the CAM-Chem model output at 0.9° × 1.25° horizontal resolution[50]. Chemical processes are assessed using the gas-phase Carbon-Bond Mechanism Z mechanism (CBMZ)[51] and the four-bin sectional Model for Simulating Aerosol Interactions and Chemistry (MOSAIC) aerosol scheme with dry diameters of 0.039–0.156, 0.156–0.625, 0.625–2.5, and 2.5–10.0 μm[52]. The SIAs formation is described in the CBMZ-MOSAIC through precursor gas oxidation (the gas-phase oxidation of SO_2/NO_x, the aqueous-phase oxidation of SO_2/NO_x in clouds, and the hydrolysis of dinitrogen pentoxide) to form H_2SO_4/HNO_3 and subsequent neutralization/condensation by/with NH_3. The thermodynamics and phase equilibrium of SIAs are simulated by the Multicomponent Taylor Expansion Method (MTEM) and a computationally efficient Multicomponent Equilibrium Solver for Aerosols (MESA) in the thermodynamic module of MOSAIC. The gas-particle equilibrium of semi-volatile components (e.g. ammonium nitrate) is determined by the Adaptive Step Time-Split Euler Method in the gas-particle partitioning module of MOSAIC[52]. We add the heterogeneous sulfate formation reactions on particle surfaces based on Chen et al.[53] to improve SIAs simulation. The Rapid Radiative Transfer Model for GCMs (RRTGM) scheme is used to parameterize shortwave and longwave radiation transfer[54]. Other physical parameterizations are the same as those used by Liu et al.[26].

Model improvement. Our model will underestimate $PM_{2.5}$ concentrations as the chemical mechanisms do not consider online secondary organic aerosol (SOA) formation due to its high uncertainty. Here we use a multiple of the OC concentrations to make up the SOA component by comparing simulated $PM_{2.5}$ components to the observations (Supplementary Fig. 2). SOA concentrations are characterized as three times that of OC in summer and two times in other months[55]. This SOA assumption has little effect on our results because SIA and SOA chemistry are decoupled in the model. In addition, to account for OC underestimates, we increase the OC concentrations in Eastern and Central European countries by two and five times, respectively.

Model emissions. Anthropogenic emissions in 2015 use the monthly estimates from the Evaluating the Climate and Air Quality Impacts of Short-Lived Pollutants (ECLIPSE) Project at 0.1° × 0.1° spatial resolution for Europe, deriving from the GAINS (Greenhouse gas and Air pollution Interactions and Synergies) model and the Emissions Database for Global Atmospheric Research (EDGARv5.0) inventory at 0.1° × 0.1° spatial resolution for regions outside Europe (https://edgar.jrc.ec.europa.eu/dataset_ap50). We further use sector-specific diurnal weighting profiles for the anthropogenic emissions from power, industry, residential, transportation, and agriculture sectors as model hourly emission inputs (Supplementary Table 4). ECLIPSE estimates of anthropogenic NO_2 and NH_3 emissions over Europe in 2015 are 3.7 Tg N and 4.4 Tg N, respectively, which are consistent with current anthropogenic emission inventories (Supplementary Table 1). NO_x emissions have high values in the Netherlands, Belgium, and other European urban areas. While the high values of NH_3 emissions are in the Netherlands, northern Germany, western France, and northern Italy (Supplementary Fig. 1). Biomass burning emissions adopt the Fire Inventory from the NCAR[56]. Biogenic emissions are estimated online using the Model of Emissions of Gases and Aerosols from Nature (MEGAN)[57], except for the soil NO_x emissions that are from the GEOS-Chem model (http://geoschemdata.wustl.edu/ExtData/HEMCO/OFFLINE_SOILNOX/).

Model sensitivity simulations. We conduct a Base simulation in 2015 and a series of sensitivity simulations to examine the impacts of Nr emission reductions on $PM_{2.5}$ air quality in Europe. First, the baseline simulation (denoted as Base) incorporates the 2015 emissions described above that have been assessed using observations. Second, a group of sensitivity simulations (denoted as S1R*N*, *N* = 30, 60, 80, and 100) reduces anthropogenic Nr emissions (both NO_x and NH_3 emissions) over Europe by 30%, 60%, 80%, and 100%, respectively. The differences in $PM_{2.5}$ concentrations between Base and S1R*N* can estimate the effects of Nr emission reductions. Third, a group of sensitivity simulations (denoted as S2R*N*, *N* = 30, 60, 80, and 100), similar to S1RN, but only reduces NO_x emissions. Fourth, another group of sensitivity simulations (denoted as S3R*N*, *N* = 30, 60, 80, and 100), similar to S1RN, but only reduces NH_3 emissions. The comparison of $PM_{2.5}$ changes between S2RN and S3RN then quantifies the respective effectiveness of NO_x and NH_3 abatement. For all simulations, typical months for the four seasons (January, April, July, and October) after a 3-day spin-up for initialization are simulated to represent yearly results due to limited computing resources.

Health-impact of Nr emission on $PM_{2.5}$

We assess the $PM_{2.5}$-related chronic health impacts through the Global Exposure Mortality Model (GEMM)[58]. It develops a $PM_{2.5}$-mortality hazard ratio function according to cohort studies of worldwide outdoor air pollution, and has been widely used in recent studies[59,60]. This concentration-response function-based method focuses on total $PM_{2.5}$ mass without assessing individual $PM_{2.5}$ components for which evidence is limited[9], corresponding with the GBD study[1]. The total health burden of long-term $PM_{2.5}$ exposure is attributed to noncommunicable diseases and lower respiratory infections (NCD and LRI). $PM_{2.5}$-related premature deaths (ΔMort) for adults (≥25 years) with age groups in 5-year intervals from 25 to greater than 85 are calculated by the following formulas:

$$RR_i(c) = \exp(\theta \times \log(\frac{z}{\alpha+1})/(1+\exp(-\frac{z-\mu}{\upsilon}))), z = \max(0, c-2.4) \quad (1)$$

$$\Delta Mort = \sum_{i=1}^{12} Base_i \times Pop_i \times \frac{1}{RR_i} \quad (2)$$

where RR_i is the relative risk of NCD or LRI for age group i (i = 1, 2,…,12), which means the contribution of $PM_{2.5}$ pollution to the baseline mortality rate; c is ambient annual $PM_{2.5}$ concentrations, exp is the natural exponential function, and θ, α, μ and υ are parameters that determine the shape of relative risk in GEMM and are specified for each age group. The $PM_{2.5}$ threshold is 2.4 μg·m^{-3}, below which no impact occurs. $Base_i$ is the baseline mortality rate of NCD or LRI for age group i, obtained from the Global Burden of Disease Study of 2015, and Pop_i is the gridded population within age group i, derived from the Gridded Population of the World version 4.11 (GPWv4) dataset. We further use the Monte Carlo method to provide the 95% confidence interval (CI) of deaths through ten thousand-time estimates.

Indicators of Nr control for $PM_{2.5}$ mitigation

Here, we apply a mass-based indicator of instant efficiency to quantify the effectiveness of Nr controls in reducing total $PM_{2.5}$ concentrations, and then use a molar-based indicator of G ratio to explain changes in the effectiveness of $PM_{2.5}$ mitigation. We calculate the efficiency of Nr emission controls based on the sensitivity simulations following the definition in Liu's (2021)[26]. The instant efficiency is defined as:

$$\beta_{LN} = \frac{\Delta[PM_{2.5}]_{LN} - \Delta[PM_{2.5}]_{L(N+1)}}{[PM_{2.5}]_{base}} \Big/ \frac{\Delta[Emi]_{LN} - \Delta[Emi]_{L(N+1)}}{[Emi]_{base}}, N = 1 \quad (3)$$

$$\beta_{LN} = \frac{\Delta[PM_{2.5}]_{L(N-1)} - \Delta[PM_{2.5}]_{L(N+1)}}{[PM_{2.5}]_{base}} \Big/ \frac{\Delta[Emi]_{L(N-1)} - \Delta[Emi]_{L(N+1)}}{[Emi]_{base}}, N = 2, 3, \ldots, 10 \quad (4)$$

$$\beta_{LN} = \frac{\Delta[PM_{2.5}]_{L(N-1)} - \Delta[PM_{2.5}]_{LN}}{[PM_{2.5}]_{base}} \Big/ \frac{\Delta[Emi]_{L(N-1)} - \Delta[Emi]_{LN}}{[Emi]_{base}}, N = 11 \quad (5)$$

where $[Emi]_{base}$ is baseline Nr emissions (in unit of Tg N), $[PM_{2.5}]_{base}$ is baseline simulated total $PM_{2.5}$ mass concentrations (in unit of μg·m^{-3}), $\Delta[Emi]_{LN}$ is the mass of Nr emissions reductions for level LN ($L1$ = 0%, $L2$ = 10%, $L3$ = 20%, …, $L10$ = 90%, and $L11$ = 100%) relative to the baseline (in unit of Tg N), and $\Delta[PM_{2.5}]_{LN}$ is associated total $PM_{2.5}$ mass decreases (in unit of μg·m^{-3}), denoting the instant response of total $PM_{2.5}$ mass in percentage to 1% mass reduction in Nr emissions under each Nr emission scenario. $PM_{2.5}$ concentrations on each 10% Nr (NO_x or NH_3) emission scenario are calculated through a shape-preserving piecewise cubic spline interpolation among the 13 sets of simulated $PM_{2.5}$ concentrations. We define the tipping point of NH_3 emission reductions as $\beta_{NH3} - \beta_{NOx} = 0$.

G ratio is applied to diagnose the availability of NH_3 in the air and to analyze the chemical regime of SIAs formation[25]. We calculate the G ratio using the equations below.

$$G = \frac{[NH_3] + [NH_4^+] - 2 \times [SO_4^{2-}]}{[HNO_3] + [NO_3^-]} \quad (6)$$

where [NH_4+], [NH_3], [H_2SO_4],[HNO_3], and [NO_3^-] are the molar concentrations (in unit of μmol·m^{-3}). Values of the G ratio below 1 mean that ammonia is insufficient to neutralize all H_2SO_4 and total nitrate, indicating an NH_3-limited chemical regime where SIAs formation is limited by the availability of NH_3[35]. In contrast, values of the G ratio above 1 mean that ammonia is sufficient to neutralize total nitrate, which characterizes a HNO_3-limited chemical regime where SIAs formation is limited by the availability of HNO_3. The G ratio of 1 means that changes (in mol units) in NH_3 and NO_x emissions can result in similar $PM_{2.5}$ changes. We note, that such diagnoses concerning SIAs formation to NH_3 and to HNO_3 availability are invalid for high temperature and low relative humidity as little ammonium nitrate aerosol is present[25].

Diagnostic diagram for Nr control pathways

The diagnostic diagram is developed for evaluating Nr control pathways targeting $PM_{2.5}$ abatement (Fig. 5). We first calculate $PM_{2.5}$ concentrations on each 10% Nr (NO_x or NH_3) emission scenario (the white circle symbols in the diagnostic diagram) through a shape-preserving piecewise cubic spline interpolation among the 13 sets of simulated regional mean $PM_{2.5}$ concentrations (the black circle symbols in the diagnostic diagram) to obtain $PM_{2.5}$ isopleths. The isopleth gradients (the blue arrows in the diagnostic diagram) are then calculated as Eq. 7 to represent the effectiveness of $PM_{2.5}$ reductions.

$$\nabla[PM_{2.5}] = \frac{\partial[PM_{2.5}]}{\partial x} \times \vec{\mathbf{i}} + \frac{\partial[PM_{2.5}]}{\partial y} \times \vec{\mathbf{j}} = \beta_{NH3} \times \vec{\mathbf{i}} + \beta_{NOx} \times \vec{\mathbf{j}} \quad (7)$$

Here x and y axes represent the strengths of the NH_3 and NO_x emission controls, respectively. $\mathbf{i}$ and $\mathbf{j}$ are unit vectors in the x-direction and y-direction, respectively. $\partial PM_{2.5}/\partial x$ is the gradient in the x-direction showing instant efficiency from NH_3 controls. $\partial PM_{2.5}/\partial y$ is the gradient in the y-direction showing instant efficiency from NO_x controls. The effectiveness diagnostic diagram can illustrate the total $PM_{2.5}$ declines by isopleths, the combined instant efficiency on $PM_{2.5}$ abatement by the size of arrows, and the relative efficiency between NH_3 and NO_x by the direction of arrows. Therefore, the optimal pathway for effective $PM_{2.5}$ declines can be found by following the isopleth gradients.

Data availability

Surface chemical measurements in Europe are obtained from the air quality database of the European Environment Agency (EEA, https://www.eea.europa.eu/data-and-maps/data/aqereporting-9). Meteorological observations are available from the National Climatic Data Center (NCDC, https://ncdc.noaa.gov/isd/data-access). Gridded population and demographic characteristics are derived from the Gridded Population of the World version 4.11 (GPWv4) dataset (https://doi.org/10.7927/H4PN93PB, https://doi.org/10.7927/H46M34XX). The baseline mortality rate of noncommunicable diseases and lower respiratory infections are obtained from the Global Burden of Disease Study (https://vizhub.healthdata.org/gbd-results/). The anthropogenic emission inventory and emission control costs are available from the corresponding author on request. The data and modeling outputs generated in this study have been deposited at https://doi.org/10.5281/zenodo.7934101[61] and are openly accessible.

Code availability

The codes of WRF-Chem version 4.0.3 are available at https://github.com/wrf-model/WRF/releases/tag/v4.0.3. Codes for calculations and data processing are written in MATLAB and are available from the corresponding author upon request.

References

1. State of Global Air 2020 (Health Effects Institute, 2020); https://www.stateofglobalair.org/.
2. Lelieveld, J., Evans, J. S., Fnais, M., Giannadaki, D. & Pozzer, A. The contribution of outdoor air pollution sources to premature mortality on a global scale. *Nature* **525**, 367–371 (2015).
3. *WHO global air quality guidelines: particulate matter (PM2.5 and PM10), ozone, nitrogen dioxide, sulfur dioxide and carbon monoxide*. (World Health Organization, 2021).
4. Reis, S. et al. From acid rain to climate change. *Science* **338**, 1153–1154 (2012).
5. Kuklinska, K., Wolska, L. & Namiesnik, J. Air quality policy in the U.S. and the EU – a review. *Atmos. Pollut. Res.* **6**, 129–137 (2015).
6. Zheng, B. et al. Trends in China's anthropogenic emissions since 2010 as the consequence of clean air actions. *Atmos. Chem. Phys.* **18**, 14095–14111 (2018).

7. Shaddick, G., Thomas, M. L., Mudu, P., Ruggeri, G. & Gumy, S. Half the world's population are exposed to increasing air pollution. *npj Clim. Atmos. Sci.* **3**, 23 (2020).
8. Air quality in Europe 2021 (European Environment Agency, 2021); https://www.eea.europa.eu//publications/air-quality-in-europe-2021.
9. Chen, J. & Hoek, G. Long-term exposure to PM and all-cause and cause-specific mortality: a systematic review and meta-analysis. *Environ. Int.* **143**, 105974 (2020).
10. Weichenthal, S. et al. How low can you go? Air pollution affects mortality at very low levels. *Sci. Adv.* **8**, eabo3381 (2022).
11. Compton, J. E. et al. Ecosystem services altered by human changes in the nitrogen cycle: a new perspective for US decision making. *Ecol. Lett.* **14**, 804–815 (2011).
12. Sutton, M. A. et al. Too much of a good thing. *Nature* **472**, 159–161 (2011).
13. Galloway, J. N. et al. The nitrogen cascade. *Bioscience* **53**, 341–356 (2003).
14. Fowler, D. et al. The global nitrogen cycle in the twenty-first century. *Philos. Trans. R. Soc. Lond. B Biol. Sci.* **368**, 20130164 (2013).
15. Erisman, J. W., Grennfelt, P. & Sutton, M. The European perspective on nitrogen emission and deposition. *Environ. Int.* **29**, 311–325 (2003).
16. Van Grinsven, H. J. et al. Costs and benefits of nitrogen for Europe and implications for mitigation. *Environ. Sci. Technol.* **47**, 3571–3579 (2013).
17. Plautz, J. Piercing the haze. *Science* **361**, 1060–1063 (2018).
18. Gu, B. et al. Abating ammonia is more cost-effective than nitrogen oxides for mitigating PM2. 5 air pollution. *Science* **374**, 758–762 (2021).
19. Daellenbach, K. R. et al. Sources of particulate-matter air pollution and its oxidative potential in Europe. *Nature* **587**, 414–419 (2020).
20. Clappier, A., Thunis, P., Beekmann, M., Putaud, J. P. & de Meij, A. Impact of SOx, NOx and NH3 emission reductions on PM2.5 concentrations across Europe: hints for future measure development. *Environ. Int.* **156**, 106699 (2021).
21. Pozzer, A., Tsimpidi, A. P., Karydis, V. A., de Meij, A. & Lelieveld, J. Impact of agricultural emission reductions on fine-particulate matter and public health. *Atmos. Chem. Phys.* **17**, 12813–12826 (2017).
22. Jimenez, J. L. et al. Evolution of organic aerosols in the atmosphere. *Science* **326**, 1525–1529 (2009).
23. Mooibroek, D., Schaap, M., Weijers, E. P. & Hoogerbrugge, R. Source apportionment and spatial variability of PM2.5 using measurements at five sites in the Netherlands. *Atmos. Environ.* **45**, 4180–4191 (2011).
24. Buczynska, A. J. et al. Composition of PM2.5 and PM1 on high and low pollution event days and its relation to indoor air quality in a home for the elderly. *Sci. Total Environ.* **490**, 134–143 (2014).
25. Ansari, A. S. & Pandis, S. N. Response of inorganic PM to precursor concentrations. *Environ. Sci. Technol.* **32**, 2706–2714 (1998).
26. Liu, Z. et al. The nonlinear response of fine particulate matter pollution to ammonia emission reductions in North China. *Environ. Res. Lett.* **16**, 034014 (2021).
27. Jonson, J. E., Fagerli, H., Scheuschner, T. & Tsyro, S. Modelling changes in secondary inorganic aerosol formation and nitrogen deposition in Europe from 2005 to 2030. *Atmos. Chem. Phys.* **22**, 1311–1331 (2022).
28. 1999 Protocol to Abate Acidification, Eutrophication and Ground-Level Ozone to the Convention on Long-range Transboundary Air Pollution, as amended on 4 May 2012. (Gothenburg, 2013).
29. Directive (EU) 2016/2284 of the European Parliament and of the Council of 14 December 2016 on the reduction of national emissions of certain atmospheric pollutants, amending Directive 2003/35/EC and repealing Directive 2001/81 (2016); http://data.europa.eu/eli/dir/2016/2284/oj.
30. McDuffie, E. E. et al. Source sector and fuel contributions to ambient PM(2.5) and attributable mortality across multiple spatial scales. *Nat. Commun.* **12**, 3594 (2021).
31. Crippa, M., Solazzo, E., Guizzardi, D., Van Dingenen, R. & Leip, A. Air pollutant emissions from global food systems are responsible for environmental impacts, crop losses and mortality. *Nat. Food* **3**, 942–956 (2022).
32. *Zero Pollution Action Plan: towards zero pollution for air, water and soil*, <https://ec.europa.eu/environment/strategy/zero-pollution-action-plan_en > (2021).
33. Erisman, J. W. & Schaap, M. The need for ammonia abatement with respect to secondary PM reductions in Europe. *Environ. Pollut.* **129**, 159–163 (2004).
34. Megaritis, A. G., Fountoukis, C., Charalampidis, P. E., Pilinis, C. & Pandis, S. N. Response of fine particulate matter concentrations to changes of emissions and temperature in Europe. *Atmos. Chem. Phys.* **13**, 3423–3443 (2013).
35. Thunis, P. et al. Non-linear response of PM2.5 to changes in NOx and NH3 emissions in the Po basin (Italy): consequences for air quality plans. *Atmos. Chem. Phys.* **21**, 9309-9327 (2021).
36. Amann, M. et al. Cost-effective control of air quality and greenhouse gases in Europe: modeling and policy applications. *Environ. Modell. Softw.* **26**, 1489–1501 (2011).
37. Winiwarter, W. & Klimont, Z. The role of N-gases (N2O, NOx, NH3) in cost-effective strategies to reduce greenhouse gas emissions and air pollution in Europe. *Curr. Opin. Environ. Sustain.* **3**, 438–445 (2011).
38. Klimont, Z. & Winiwarter, W. *Estimating costs and potential for reduction of ammonia emissions from agriculture in the GAINS model*. In *Costs of ammonia abatement and the climate co-benefits* 233–261 (Springer, 2015).
39. Amann, M. et al. An updated set of scenarios of cost-effective emission reductions for the revision of the Gothenburg Protocol. *CIAM Rep.* **4**, 2011 (2011).
40. Gu, B. et al. Cost-effective mitigation of nitrogen pollution from global croplands. *Nature* **613**, 77–84 (2023).
41. Galloway, J. N. et al. Transformation of the nitrogen cycle: recent trends, questions, and potential solutions. *Science* **320**, 889–892 (2008).
42. Liu, X. et al. Enhanced nitrogen deposition over China. *Nature* **494**, 459–462 (2013).
43. Yang, A. L. et al. Policies to combat nitrogen pollution in South Asia: gaps and opportunities. *Environ. Res. Lett.* **17**, 025007 (2022).
44. Pai, S. J., Carter, T. S., Heald, C. L. & Kroll, J. H. Updated World Health Organization Air Quality Guidelines Highlight the Importance of Non-anthropogenic $PM_{2.5}$. *Environ. Sci. Technol. Lett.* **9**, 501–506 (2022).
45. Zheng, G. et al. Multiphase buffer theory explains contrasts in atmospheric aerosol acidity. *Science* **369**, 1374–1377 (2020).
46. Lv, S. et al. Gas-to-aerosol phase partitioning of atmospheric water-soluble organic compounds at a rural site in China: an enhancing effect of NH3 on SOA formation. *Environ. Sci. Technol.* **56**, 3915–3924 (2022).
47. Bash, J. O., Cooter, E. J., Dennis, R. L., Walker, J. T. & Pleim, J. E. Evaluation of a regional air-quality model with bidirectional NH3 exchange coupled to an agroecosystem model. *Biogeosciences* **10**, 1635–1645 (2013).
48. Zhu, L. et al. Global evaluation of ammonia bidirectional exchange and livestock diurnal variation schemes. *Atmos. Chem. Phys.* **15**, 12823–12843 (2015).
49. Hersbach, H. et al. *ERA5 hourly data on pressure levels from 1959 to present. Copernicus Climate Change Service (C3S) Climate Data Store (CDS)*. https://doi.org/10.24381/cds.bd0915c6 (2018).

50. Buchholz, R., Emmons, L., Tilmes, S. & Team, T. CESM2. 1/CAM-chem instantaneous output for boundary conditions. *UCAR/NCAR-Atmospheric Chemistry Observations and Modeling Laboratory*. https://doi.org/10.5065/NMP7-EP60 (2019).
51. Zaveri, R. A. & Peters, L. K. A new lumped structure photochemical mechanism for large-scale applications. *J. Geophys. Res.: Atmos.* **104**, 30387–30415 (1999).
52. Zaveri, R. A., Easter, R. C., Fast, J. D. & Peters, L. K. Model for Simulating Aerosol Interactions and Chemistry (MOSAIC). *J. Geophys. Res.* **113**, D13204 (2008).
53. Chen, D., Liu, Z., Fast, J. & Ban, J. Simulations of sulfate–nitrate–ammonium (SNA) aerosols during the extreme haze events over northern China in October 2014. *Atmos. Chem. Phys.* **16**, 10707–10724 (2016).
54. Iacono, M. J. et al. Radiative forcing by long-lived greenhouse gases: Calculations with the AER radiative transfer models. *J. Geophys. Res.: Atmos.* **113**, D13103 (2008).
55. Chen, G. et al. European aerosol phenomenology-8: harmonised source apportionment of organic aerosol using 22 year-long ACSM/AMS datasets. *Environ. Int.* **166**, 107325 (2022).
56. Wiedinmyer, C. et al. The Fire INventory from NCAR (FINN): a high resolution global model to estimate the emissions from open burning. *Geosci. Model Dev.* **4**, 625–641 (2011).
57. Guenther, A. et al. Estimates of global terrestrial isoprene emissions using MEGAN (Model of Emissions of Gases and Aerosols from Nature). *Atmos. Chem. Phys.* **6**, 3181–3210 (2006).
58. Burnett, R. et al. Global estimates of mortality associated with long-term exposure to outdoor fine particulate matter. *Proc. Natl. Acad. Sci. USA* **115**, 9592–9597 (2018).
59. Geng, G. et al. Drivers of PM2.5 air pollution deaths in China 2002–2017. *Nat. Geosci.* **14**, 645–650 (2021).
60. Zhou, M. et al. Environmental benefits and household costs of clean heating options in northern China. *Nat. Sustain.* **5**, 329–338 (2022).
61. Zehui Liu, Harald Rieder, Wilfried Winiwarter, & Lin Zhang. Dataset for Optimal reactive nitrogen control pathways identified for cost-effective PM2.5 mitigation in Europe. *Zenodo*. https://doi.org/10.5281/zenodo.7934101 (2023).

Acknowledgements

The work was supported by the UNCNET project, a project funded under the JPI Urban Europe/China collaboration, Project Numbers 71961137011 (NSFC, China), UMO-2018/29/Z/ST10/02986 (NCN, Poland), and 870234 (FFG, Austria). Z.L. acknowledges funds from the China Scholarship Council.

Author contributions

L.Z., Z.L., and W.W. designed the research. Z.L. performed the research. L.Z., W.W., and H.R. helped with results interpretation. Z.L. and W.W. processed the European emission estimates and emission control costs. Z.L., H.R., C.S., and M.M. contributed to air-quality modeling. W.W., H.R., and L.Z. helped develop diagnostic diagram for Nr control pathways. Z.L., W.W., L.Z., and Y.G. wrote the paper with input from all the co-authors.

Competing interests

The authors declare no competing interests.

Additional information

Supplementary information The online version contains supplementary material available at https://doi.org/10.1038/s41467-023-39900-9.

Correspondence and requests for materials should be addressed to Wilfried Winiwarter or Lin Zhang.

Peer review information *Nature Communications* thanks the anonymous reviewers for their contribution to the peer review of this work.